For initial state II, however, the entanglement behaves very differently: The concurrence goes to zero for $p < 1$, thus demonstrating "entanglement sudden death." We stress that the onset of separability ($C = 0$) occurs at the same point for all entanglement quantifiers and is not a particular artifact of the concurrence.

It is also illustrative to study the purity, defined as $\mathrm{tr}\rho^2$, as a function of the decay probability (Fig. 3) for states I and II. In both cases the purity reaches a minimum but is restored when $p = 1$, when all photons have "decayed" to the H-polarization state. State II is more mixed than state I in the intermediate stages of this process because it has a larger $|VV\rangle$ component and thus becomes more entangled with the environment.

To further illustrate the usefulness of the present scheme for studying decoherence of entangled systems, we performed a second experiment studying the phase-damping channel, described by the map (*1*):

$$|g\rangle_S\otimes|0\rangle_R \rightarrow |g\rangle_S\otimes|0\rangle_R$$
$$|e\rangle_S\otimes|0\rangle_R \rightarrow \sqrt{1-p}|e\rangle_S\otimes|0\rangle_R + \sqrt{p}|e\rangle_S\otimes|1\rangle_R \quad (6)$$

This map could represent elastic scattering between atom and reservoir. States $|e\rangle$ and $|g\rangle$ are not changed by the interaction, but any coherent superposition of them gets entangled with the reservoir. There is no longer decay, but only loss of coherence between ground and excited states. The dephasing map can be implemented with the same interferometer through the addition of an extra HWP at 45° in mode b before the QST system (or, equivalently, through the removal of HWP3 and redefinition of the QST measurements). For the dephasing channel, pure states I and II present identical behavior, becoming completely disentangled only when $p = 1$. Figure 4 shows the concurrence (squares) and bipartite purity (triangles) as a function of p for the entangled state II.

In demonstrating the sudden disappearance of the entanglement of a bipartite system, induced by the interaction with an environment, our results show that entangled states with the same initial concurrence may exhibit, for the same reservoir, either an abrupt or an asymptotic disappearance of entanglement, even though the constituents of the system always exhibit an asymptotic decay. We have explicitly shown that this behavior also depends on the characteristics of the reservoir through two examples corresponding to amplitude decay and dephasing. The experimental setup represents a reliable and simple method for studying the dynamics of entangled systems interacting with controlled environments.

References and Notes

1. M. Nielsen, I. Chuang, *Quantum Computation and Quantum Information* (Cambridge Univ. Press, Cambridge, 2000).
2. C. H. Bennett, D. P. DiVincenzo, *Nature* **404**, 247 (2000).
3. C. H. Bennett, G. Brassard, *Proceedings of the International Conference on Computer Systems and Signal Processing, Bangalore, India* (IEEE, New York, 1984), pp. 175–179.
4. A. K. Ekert, *Phys. Rev. Lett.* **67**, 661 (1991).
5. N. Gisin, G. Ribordy, W. Tittel, H. Zbinden, *Rev. Mod. Phys.* **74**, 145 (2002).
6. C. H. Bennett *et al.*, *Phys. Rev. Lett.* **70**, 1895 (1993).
7. D. Bouwmeester *et al.*, *Nature* **390**, 575 (1997).
8. D. Boschi, S. Branca, F. DeMartini, L. Hardy, S. Popescu, *Phys. Rev. Lett.* **80**, 1121 (1998).
9. L.-M. Duan, M. D. Lukin, J. I. Cirac, P. Zoller, *Nature* **414**, 413 (2001).
10. W. H. Zurek, *Rev. Mod. Phys.* **75**, 715 (2003).
11. L. Diósi, in *Irreversible Quantum Dynamics*, F. Benatti, R. Floreanini, Eds. (Springer, Berlin, 2003), pp. 157–164.
12. P. J. Dodd, J. J. Halliwell, *Phys. Rev. A* **69**, 052105 (2004).
13. T. Yu, J. H. Eberly, *Phys. Rev. Lett.* **93**, 140404 (2004).
14. M. F. Santos, P. Milman, L. Davidovich, N. Zagury, *Phys. Rev. A* **73**, 040305 (2006).
15. T. Yu, J. H. Eberly, *Phys. Rev. Lett.* **97**, 140403 (2006).
16. W. K. Wootters, *Phys. Rev. Lett.* **80**, 2245 (1998).
17. A similar configuration, but with the addition of cylindrical lenses, was used to realize a direct measurement of entanglement for a pure state in (*21*).
18. D. F. V. James, P. G. Kwiat, W. J. Munro, A. G. White, *Phys. Rev. A* **64**, 052312 (2001).
19. P. G. Kwiat, E. Waks, A. G. White, I. Appelbaum, P. H. Eberhard, *Phys. Rev. A* **60**, R773 (1999).
20. J. B. Altepeter, E. R. Jeffrey, P. G. Kwiat, in *Advances in Atomic, Molecular and Optical Physics*, P. Berman, C. Lin, Eds. (Elsevier, San Diego, CA, 2005), vol. 52, pp. 107–161.
21. S. P. Walborn, P. H. S. Ribeiro, L. Davidovich, F. Mintert, A. Buchleitner, *Nature* **440**, 1022 (2006).

22. Supported by the Brazilian funding agencies CNPq, CAPES, PRONEX, FUJB, and FAPER]. This work was performed as part of the Brazilian Millennium Institute for Quantum Information.

12 January 2007; accepted 20 March 2007
10.1126/science.1139892

Enantioselective Organocatalysis Using SOMO Activation

Teresa D. Beeson,[1,2] Anthony Mastracchio,[1,2] Jun-Bae Hong,[1,2] Kate Ashton,[1,2] David W. C. MacMillan[1,2]*

The asymmetric α-addition of relatively nonpolar hydrocarbon substrates, such as allyl and aryl groups, to aldehydes and ketones remains a largely unsolved problem in organic synthesis, despite the wide potential utility of direct routes to such products. We reasoned that well-established chiral amine catalysis, which activates aldehydes toward electrophile addition by enamine formation, could be expanded to this important reaction class by applying a single-electron oxidant to create a transient radical species from the enamine. We demonstrated the concept of singly occupied molecular orbital (SOMO) activation with a highly selective α-allylation of aldehydes, and we here present preliminary results for enantioselective heteroarylations and cyclization/halogenation cascades.

Over the past four decades, the capacity to induce asymmetric transformations with enantioselective catalysts has remained a focal point for extensive research efforts in both industrial and academic settings. During this time, thousands of asymmetric catalytic reactions have been invented (*1*), in accord with the increasing need for enantiopure medicinal agents and the rapid advancement of the field of asymmetric synthesis. Most catalytic enantioinductive processes are derived from a small number of long-established activation modes. Activation modes such as Lewis acid catalysis (*2*), σ-bond insertion (*3*), π-bond insertion (*4*), atom transfer catalysis (*5*), and hydrogen bonding catalysis (*6*) have each spawned countless asymmetric reaction classes, thereby dramatically expanding the synthetic toolbox available to researchers in the physical and biological sciences. A necessary objective, therefore, for the continued advancement of the field of chemical synthesis is the design and implementation of distinct catalytic-activation modes that enable previously unknown transformations.

Over the past 8 years, our laboratory has been involved in the development of the field of organocatalysis, a research area that relies on the use of small organic molecules as catalysts for enantioselective transformations. As part of these studies, we introduced the concept of iminium catalysis (*7*): an enal or enone activation mode that lowers the energy of the substrate's lowest unoccupied molecular orbital, facilitating enantioselective C–C and C–N conjugate additions, cycloadditions, hydrogenations, and Friedel-Crafts alkylations (*8*). Simultaneously, Barbas and List (*9*) brought to fruition the concept of enamine catalysis (Fig. 1), which raises the energy of the highest occupied molecular orbital (HOMO) in aldehydes and ketones to promote enantioselective α-carbonyl functionalization with a large range of electrophiles (*10*). These two modes of catalyst activation (iminium and enamine) have provided, in total, more than 60 asymmetric methodologies over the past 7 years.

[1]Merck Center for Catalysis, Department of Chemistry, Princeton University, Princeton, NJ 08544, USA. [2]Division of Chemistry and Chemical Engineering, California Institute of Technology, Pasadena, CA 91125, USA.

*To whom correspondence should be addressed. E-mail: dmacmill@princeton.edu

Given the established capacity of enamines and iminium ions to rapidly interconvert via a redox process (enamine has four π electrons and iminium has two π electrons), we recently questioned whether it might be possible to interrupt this equilibrium chemically and thereby to access a mode of catalytic activation that electronically bisects enamine and iminium formation. More specifically, we hypothesized that a one-electron oxidation of a transient enamine species (Fig. 2A) should generate a three–π-electron radical cation with a singly occupied molecular orbital (SOMO) that is activated toward a range of enantioselective catalytic transformations not currently possible with established catalysis concepts.

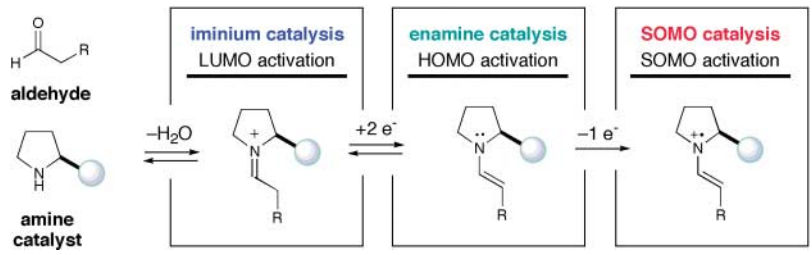

Fig. 1. SOMO catalysis via single-electron oxidation of a transiently formed enamine. LUMO, lowest unoccupied molecular orbital; R, an arbitrary organic substituent.

Table 1. Representative SOMO catalysis. Enantioselective aldehyde α-allylation is shown. Bz, benzoyl; Boc, *tert*-butyl carbamoyl; Et, ethyl.

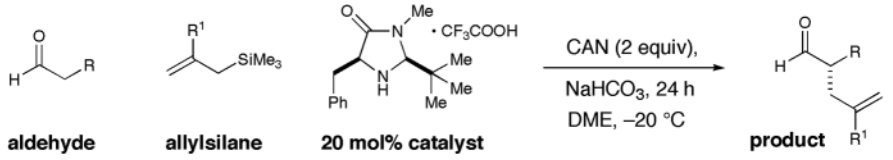

entry	aldehyde	product*	entry	aldehyde	product*
1	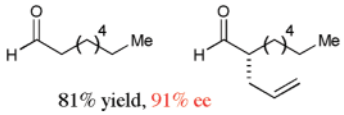	81% yield, 91% ee	4	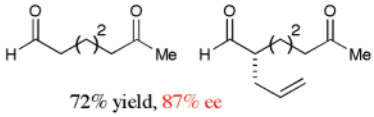	72% yield, 87% ee
2	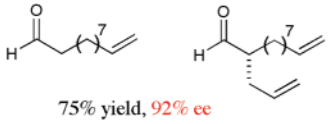	75% yield, 92% ee	5	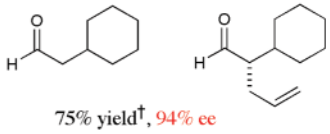	75% yield†, 94% ee
3	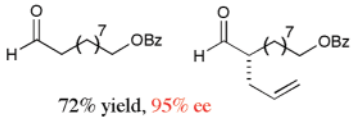	72% yield, 95% ee	6	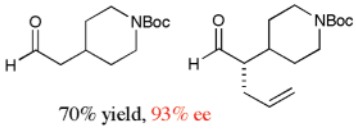	70% yield, 93% ee

entry	allylsilane	product‡	entry	allylsilane	product‡
7	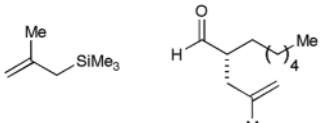	88% yield, 91% ee	9	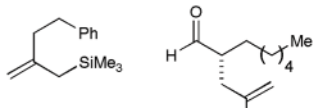	77% yield, 88% ee
8	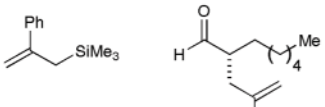	87% yield, 90% ee	10	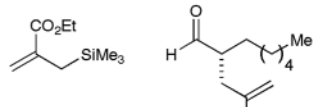	81% yield, 90% ee

*Reactions performed with allylsilane (CH_2=$CHCH_2SiMe_3$). †Yield determined by gas chromatographic analysis. ‡Reactions performed with octanal.

From the outset, we identified three key design elements to substantiate this proposal. First, we recognized the mechanistic requirement that an equilibrium population of enamine must undergo selective oxidation in the presence of an amine catalyst, an aldehyde substrate, and an iminium ion precursor. Theoretical support for such a chemoselective pathway was derived from the ionization potentials (IPs) of 1-(but-1-enyl)pyrrolidine (IP = 7.2 eV), pyrrolidine (IP = 8.8 eV), and butanal (IP = 9.8 eV)—data that reveal the transient enamine component to be sufficiently more susceptible to oxidation than the accompanying reaction partners (*11*, *12*).

Second, we understood that the widespread application of SOMO catalysis would require the identification of an amine catalyst that could generically enforce high levels of enantiocontrol in the coupling of the pivotal radical cation with a variety of π-rich nucleophiles. On the basis of density functional theory (DFT) calculations (*13*, *14*), we proposed that the imidazolidinone catalyst **1** (*8*) should selectively form a SOMO-activated cation, DFT-**2**, that projects the three–π-electron system away from the bulky tert-butyl group, while the radical-centered carbon selectively populates an E configuration to minimize nonbonding interactions with the imidazolidinone ring (Fig. 2B). In terms of enantiofacial discrimination, the calculated DFT-**2** structure also reveals that the benzyl group on the catalyst system should effectively shield the *re* face of the radical cation, leaving the *si* face exposed for enantioselective bond formation.

Third, we knew that the intrinsic value of this activation mode would be defined by its capacity to enable useful enantioselective reactions. Radical cations show great potential in this vein, because they already participate in many noncatalytic C–C, C–O, C–N, C–S, and C–X (where X is a halogen) bond formations (*15*–*19*). Our analysis reveals the attractive prospect of applying asymmetric SOMO catalysis to important problems such as direct and enantioselective allylic alkylation, enolation, arylation, carbo-oxidation, vinylation, alkynylation, or intermolecular alkylation of aldehydes.

To test this activation concept, we selected the direct and enantioselective allylic alkylation of aldehydes as a representative transform (*20*, *21*). We recognized that the accompanying allylation products have been established as important chiral synthons in chemical synthesis (*22*, *23*). Experimentally, this allylation protocol was first examined in dimethoxy ethane (DME) solvent with octanal, imidazolidinone catalyst **1**,

ceric ammonium nitrate (CAN) as the stoichiometric oxidant, and allyltrimethylsilane as the SOMO nucleophile (Table 1) (*24*). Preliminary studies revealed the successful execution of our design ideas to provide (*R*)-2-allyl-octanal with excellent levels of enantioinduction and in good conversion [Table 1, entry 1; 81% yield, 91% enantiomeric excess (ee)]. Experiments that probed the scope of the aldehyde component in this reaction are summarized in Table 1, entries 1 to 6. There appears to be substantial latitude in the steric demand of the radical-cation substituent (compare entries 1 and 5, with the substituent being hexyl versus cyclohexyl), allowing access to a broad variety of 2-alkyl-substituted-4-pentenals (75 to 81% yield, 91 to 94% ee). Moreover, a variety of chemical functionalities appear to be inert under these mild oxidative conditions, including olefins, ketones, esters, and carbamates (entries 2 to 4 and 6; 70 to 75% yield, 87 to 95% ee).

Additionally, Table 1 reveals that a diverse array of π-rich olefinic silanes (*25*) will readily participate as allylic alkylating reagents in this catalytic protocol (entries 1 and 7 to 10). For example, methyl, phenyl, and 2-alkyl substituted allylsilanes can be tolerated without losses in reaction efficiency or enantiocontrol (entries 7 to 9; 77 to 88% yield, 88 to 91% ee). The electron-deficient olefin ethyl-2-(methyl-trimethylsilyl)-acrylate also functions effectively as a SOMO nucleophile to provide the corresponding alkylated adduct in 81% yield and 90% ee (entry 10). This last result provides circumstantial evidence for the generation and participation of a radical-cation species, given the capacity of ethyl-2-(methyl-trimethylsilyl)-acrylate to function as a viable SOMO nucleophile on account of the captodative effect (*26*), yet not as effectively as a HOMO nucleophile because of diminished π density at the olefin terminus. The sense of asymmetric induction observed in all cases (Table 1) is consistent with selective engagement of the allylsilane substrate with the *si* face of the SOMO-activated species **2**, in complete accord with the calculated structure DFT-**2**.

A survey of reaction media for this organocatalytic allylation has revealed that a variety of solvents may be used without a substantial loss in reaction efficiency, provided that water is present as an addend (*27*). Although the use of DME provides optimal selectivity, reaction rate, and chemical yield (*28*), acetone can often be used as an alternative solvent without allylation of the bulk medium (*29*). Moreover, extended reaction times do not lead to product epimerization or the formation of α,α-diallylaldehydes or aldehyde dimerization adducts.

To highlight the anticipated broad scope of SOMO activation, we present preliminary results for the enantioselective α-heteroarylation of aldehydes (Fig. 3A). Specifically, exposure of octanal and *N*-tert-butyl carbamoyl pyrrole to our SOMO activation conditions enables formyl α-arylation with useful levels of enantioselectivity and excellent yields. Moreover, we have found that unsaturated aldehydes rapidly undergo enantioselective cyclization with trapping of an exogenous halide. As revealed in Fig. 3B, activation of *cis*-6-nonenal with our SOMO protocol in the presence of LiCl leads to the formation of a stereochemically dense cyclopentyl ring system with excellent stereocontrol [85% yield, ≥10:1 diastereomeric ratio (dr), 95% ee]. This latter result again provides circumstantial evidence for the generation and participation of a radical-cation species, given the propensity of radicals to undergo cyclization with unactivated olefins.

We have undertaken studies to more definitively investigate the participation of the putative radical-cation intermediate in this catalytic process. Specifically, aldehyde activation-addition experiments were performed with the vinyl cyclopropane substrate **3**, an established radical clock that was designed by Newcomb *et al.* (*30*) to differentiate between radical-mediated pathways and cationic mechanisms (Fig. 3C). Addition of the activated aldehyde intermediate to the olefin **3** occurs with subsequent scission of the benzylic cyclopropyl bond and not the α-methoxy cyclopropyl bond. This result is in complete accord with a radical pathway and not a cationic addition mechanism.

These results highlight the substantial scope of SOMO activation for useful transformations in organic synthesis. We anticipate a wide range of applications for pharmaceutically important compounds and intermediates. After our initial submission of this work, a similar approach was also applied to aldehyde α-oxidation (*31*).

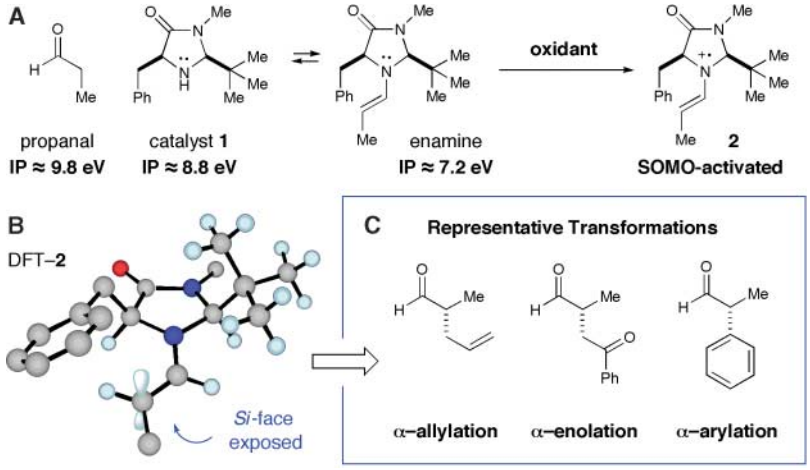

Fig. 2. (**A**) Catalytic chemical steps leading to formation of the SOMO-activated intermediate. Me, methyl; Ph, phenyl. (**B**) DFT–calculated three-dimensional structure of the enantio-differentiated radical cation. (**C**) Possible transformations arising from enantioselective organocatalytic SOMO catalysis.

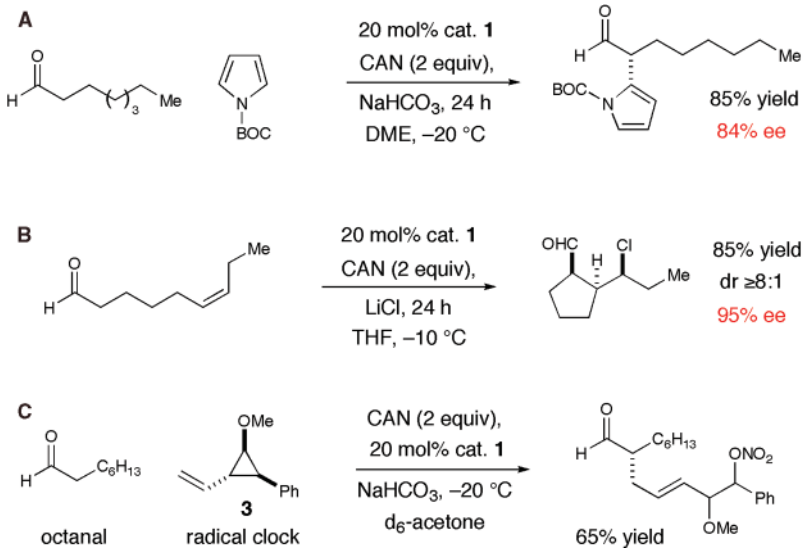

Fig. 3. (**A**) Enantioselective α-heteroarylation of aldehydes via SOMO catalysis. CAN, ceric ammonium nitrate. (**B**) Enantioselective olefin cyclization via SOMO catalysis. THF, tetrahydrofuran. (**C**) Mechanistic investigation to determine the intermediacy of a radical cation versus a carbocation.

References and Notes

1. E. N. Jacobsen, A. Pfaltz, H. Yamamoto, Eds., *Comprehensive Asymmetric Catalysis* (Springer, Berlin, 1999), vol. 1 to 3.
2. H. Yamamoto, Ed., *Lewis Acids in Organic Synthesis* (Wiley-VCH, New York, 2000).
3. R. H. Crabtree, *The Organometallic Chemistry of the Transition Metals* (Wiley-Interscience, Hoboken, NJ, ed. 4, 2005).
4. R. Noyori, in *Asymmetric Catalysis in Organic Synthesis* (Wiley-Interscience, New York, 1994), pp. 123–173.
5. I. Ojima, Ed., in *Catalytic Asymmetric Synthesis* (Wiley-VHC, New York, ed. 2, 2000), chap. 6.
6. M. S. Taylor, E. N. Jacobsen, *Angew. Chem. Int. Ed.* **45**, 1520 (2006).
7. K. A. Ahrendt, C. J. Borths, D. W. C. MacMillan, *J. Am. Chem. Soc.* **122**, 4243 (2000).
8. G. Lelais, D. W. C. MacMillan, *Aldrichim. Acta* **39**, 79 (2006) and references therein.
9. B. List, R. A. Lerner, C. F. Barbas III, *J. Am. Chem. Soc.* **122**, 2395 (2000).
10. B. List, *Chem. Commun.* **2006**, 819 (2006) and references therein.
11. K. Müller, F. Previdoli, H. Desilvestro, *Helv. Chim. Acta* **64**, 2497 (1981).
12. D. R. Lide, Ed., in *Handbook of Chemistry and Physics* (CRC Press, New York, ed. 76, 1995), pp. 220–221.
13. DFT calculations were performed at the B3LYP/6-311+G(2d,p)//B3LYP/6-31G(d) level of theory using Gaussian 03 software (*14*).
14. M. J. Frisch *et al.*, Gaussian 03 software (Gaussian, Wallingford, CT, 2004).
15. K. Narasaka, T. Okauchi, K. Tanaka, M. Murakami, *Chem. Lett. (Jpn.)* **92**, 2099 (1992).
16. M. Kirchgessner, K. Sreenath, K. R. Gopidas, *J. Org. Chem.* **71**, 9849 (2006).
17. A. Sutterer, K. D. Moeller, *J. Am. Chem. Soc.* **122**, 5636 (2000).
18. H. B. Lee, M. J. Sung, S. C. Blackstock, J. K. Cha, *J. Am. Chem. Soc.* **123**, 11322 (2001).
19. P. Renaud, M. P. Sibi, Eds., *Radicals in Organic Synthesis* (Wiley-VHC, Weinheim, Germany, 2001), vol. 2, pp. 144–205.
20. Organocatalysis in combination with organometallic catalysis has previously been applied to the nonasymmetric allylation of aldehydes.
21. I. Ibrahem, J. A. Córdova, *Angew. Chem. Int. Ed.* **45**, 1952 (2006).
22. B. M. Trost, M. L. Crawley, *Chem. Rev.* **103**, 2921 (2003).
23. J. Seyden-Penne, in *Chiral Auxiliaries and Ligands in Asymmetric Synthesis* (Wiley-Interscience, New York, 1995), pp. 166–195.
24. Materials and methods are available as supporting online material on *Science* Online.
25. Mechanistically, we speculate that addition of the π-rich allylsilane to the radical-cation species results in the formation of a β-silyl radical that undergoes rapid oxidation to the corresponding β-silyl cation before silyl elimination with concomitant olefin formation.
26. H. G. Viehe, R. Merényi, Z. Janousek, *Pure Appl. Chem.* **60**, 1635 (1988).
27. The introduction of 1 to 5 equivalents of water is required to achieve useful levels of reaction efficiency in most solvents (e.g., ethyl acetate, tetrahydrofuran, and CH_2Cl_2).
28. Bench-grade DME was found to contain sufficient water to achieve optimal results. The exclusion of water by the use of rigorously dried DME results in substantially lower chemical yields.
29. The coupling of octanal with allylsilane using acetone as the bulk medium provided the corresponding allylation product in 79% ee (75% conversion after 24 hours).
30. M.-H. Le Tadic-Biadatti, M. Newcomb, *J. Chem. Soc. Perkin Trans.* **2**, 1467 (1996).
31. M. P. Sibi, M. Hasegawa, *J. Am. Chem. Soc.* **129**, 395 (2007); published online 16 March 2007 (10.1021/ja069245n).

32. We thank R. A. Pascal for invaluable assistance in performing Gaussian DFT calculations and M. Amatore for a late-stage experimental contribution. Financial support was provided by NIH National Institute of General Medical Sciences (grant R01 GM078201-01-01) and by gifts from Amgen, Merck Research Laboratories, and the Astellas Foundation USA. T.D.B. is grateful for a Novartis predoctoral fellowship, J.-B.H. is grateful for a KRF postdoctoral fellowship, and K.A. is grateful for a Merck overseas postdoctoral fellowship.

Supporting Online Material

www.sciencemag.org/cgi/content/full/1142696/DC1
Materials and Methods
References and Notes

20 February 2007; accepted 20 March 2007
Published online 29 March 2007;
10.1126/science.1142696
Include this information when citing this paper.

A Dinuclear Ni(μ-H)Ru Complex Derived from H_2

Seiji Ogo,[1]* Ryota Kabe,[1,2] Keiji Uehara,[2] Bunsho Kure,[1,2] Takashi Nishimura,[2] Saija C. Menon,[2] Ryosuke Harada,[1] Shunichi Fukuzumi,[2] Yoshiki Higuchi,[3] Takashi Ohhara,[4] Taro Tamada,[4] Ryota Kuroki[4]

Models of the active site in [NiFe]hydrogenase enzymes have proven challenging to prepare. We isolated a paramagnetic dinuclear nickel-ruthenium complex with a bridging hydrido ligand from the heterolytic cleavage of H_2 by a dinuclear NiRu aqua complex in water under ambient conditions (20°C and 1 atmosphere pressure). The structure of the hexacoordinate Ni(μ-H)Ru complex was unequivocally determined by neutron diffraction analysis, and it comes closest to an effective analog for the core structure of the proposed active form of the enzyme.

Hydrogenases are bacterial enzymes that catalyze the activation of H_2 into two protons (H^+) and two electrons (e^-) (*1*–*3*). Hydrogen isotope exchange experiments implicate as a first step the heterolytic cleavage of H_2 into a proton and a hydride ion (H^-) (*1*–*3*). Hydrogenases are classified into two major families on the basis of the metal content of their respective dinuclear active sites—that is, [FeFe]hydrogenases (*4*) and [NiFe]hydrogenases (*5*, *6*). Recent progress toward the structures and function of the hydrogenases has been provided by x-ray analysis, spectroscopic techniques, theoretical methods, and model studies (*7*).

X-ray crystallographic studies have shown that the resting-state core structure of [NiFe]hydrogenase from *Desulfovibrio gigas* consists of one nickel atom and one iron atom, which are bridged by two cysteic thiolates and one unidentified ligand (depicted as X in Fig. 1) (*2*, *5*, *6*). The bridging ligand X in the resting state is proposed to be an oxygen ligand such as H_2O, OH^-, or O^{2-} (*8*). The role of metal atoms and bridging S and X ligands in the H_2 cleavage has so far been the subject of controversy (*8*).

Many synthetic modeling efforts have been devoted to elucidating the core structure of the active form of the [NiFe]hydrogenase, such as preparation of [NiRu]complexes by Rauchfuss and others (*9*–*15*). A Ni(μ-S)$_2$(μ-H)Fe species is one of the candidates for the active form (*1*, *5*, *16*, *17*). However, ^{10}M(μ-S)$_2$(μ-H)^{8}M complexes [where ^{10}M = group 10 metals (Ni, Pd, and Pt) and ^{8}M = group 8 metals (Fe, Ru, and Os)] as models for the active form of the [NiFe]hydrogenase have yet to be reported.

Here, we report the successful isolation and crystal structure of the paramagnetic Ni(μ-H)Ru complex $[(Ni^{II}L)(H_2O)(\mu\text{-}H)Ru^{II}(\eta^6\text{-}C_6Me_6)](NO_3)$ {[**2**](NO$_3$)}, where L = *N*,*N*′-dimethyl-*N*,*N*′-bis(2-mercaptoethyl)-1,3-propanediamine, which we synthesized by reaction of a diamagnetic dinuclear NiRu aqua complex $[(Ni^{II}L)Ru^{II}(H_2O)(\eta^6\text{-}C_6Me_6)](NO_3)_2$ {[**1**](NO$_3$)$_2$} with H_2 in water under ambient conditions (20°C and 0.1 MPa) (Fig. 2).

We obtained the highly water-soluble NiRu aqua complex [**1**](SO$_4$) by reaction of the ruthenium triaqua complex [Ru(η^6-C$_6$Me$_6$)(H$_2$O)$_3$](SO$_4$)

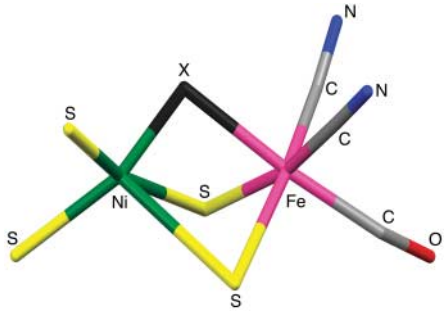

Fig. 1. Core structure of the resting form of [NiFe]hydrogenase from *D. gigas*, determined by x-ray analysis. [Adapted from (*6*)]

[1]Center for Future Chemistry, Kyushu University, Fukuoka 819–0395, Japan. [2]Department of Material and Life Science, Division of Advanced Science and Biotechnology, Graduate School of Engineering, Osaka University, Solution-Oriented Research for Science and Technology, Japan Science and Technology Agency (JST), Suita, Osaka 565–0871, Japan. [3]Department of Life Science, Graduate School of Life Science, University of Hyogo, Koto, Kamigori, Hyogo 678–1297, Japan. [4]Research Group for Molecular Structural Biology, Quantum Beam Science Directorate, Japan Atomic Energy Agency, Tokai, Ibaraki 319–1195, Japan.

*To whom correspondence should be addressed. E-mail: ogo-tcm@mbox.nc.kyushu-u.ac.jp